LabAnimal

REVIEW ARTICLE

https://doi.org/10.1038/s41684-019-0326-6

Digging deeper: methodologies for high-content phenotyping in *Caenorhabditis elegans*

Dhaval S. Patel[1,3], Nan Xu[1,2,3] and Hang Lu[1*]

Deep phenotyping is an emerging conceptual paradigm and experimental approach aimed at measuring and linking many aspects of a phenotype to understand its underlying biology. To date, deep phenotyping has been applied mostly in cultured cells and used less in multicellular organisms. However, in the past decade, it has increasingly been recognized that deep phenotyping could lead to a better understanding of how genetics, environment and stochasticity affect the development, physiology and behavior of an organism. The nematode *Caenorhabditis elegans* is an invaluable model system for studying how genes affect a phenotypic trait, and new technologies have taken advantage of the worm's physical attributes to increase the throughput and informational content of experiments. Coupling of these technical advancements with computational and analytical tools has enabled a boom in deep-phenotyping studies of *C. elegans*. In this Review, we highlight how these new technologies and tools are digging into the biological origins of complex, multidimensional phenotypes.

One of the great drivers of biological research in the twentieth century was the desire to understand how information encoded in an organism's genome gives rise to its physical and behavioral phenotypes, which are collectively referred to as its phenome[1]. However, the phenotype of an organism is not merely a reflection of its genes, but the integrated product of its genotype interacting with the environmental conditions and stochastic effects to which the individual is exposed before observation[2,3]. Consequently, an organism's phenome contains a large, multidimensional set of observable characteristics, and the phenospace in a population of individuals is vast. Understanding the specific contribution of the genome, environment and stochastic processes to the position of an individual in the phenospace is a formidable technical challenge. Fortunately, technological innovation is beginning to provide the tools necessary for quantifying these multidimensional characteristics and their underlying causes, opening up a new experimental paradigm known as deep phenotyping[4]. Considering that it is fairly new, the term deep phenotyping is broadly used within the scientific literature. In this Review, we define deep phenotyping as the coupling of high-throughput experimental techniques with computational analyses to enable the generation, examination and interpretation of high-dimensional biological data.

C. elegans has many attributes that make this organism an ideal model system for deep-phenotyping studies. The worm is a small poikilotherm with an adult body length of approximately 1 mm that feeds on bacteria; it has a rapid life cycle, developing from egg to reproductive adult in approximately 3 days at 20 °C, and it has a deterministic developmental lineage[5]. In addition, the worm primarily reproduces as a self-fertilizing hermaphrodite, which means that large, near-isogenic populations can be grown in highly controlled environmental conditions. Additionally, because at least 38% of the protein-coding genes in the worm genome have a human ortholog[6], insights gained from worm studies can inform us about human biology. Genes involved in apoptosis[7] and axonal migration[8,9], microRNAs[10,11], and RNA interference (RNAi)[12], for instance, were all initially identified in *C. elegans* and have since been shown to have roles in human disease[13–15].

In this Review, we outline the technological and analytical developments that have enabled deep-phenotyping studies in *C. elegans*. We then examine with several examples how these tools have yielded greater insight into the biology of complex phenotypes. Finally, we offer a prospective outlook on the future of deep-phenotyping experiments in *C. elegans* and in other systems.

Tools and techniques for deep phenotyping

Historically, the phenotypic analysis of *C. elegans* involved the manual measurement of morphometric or behavioral features such as changes in body shape or defects in movement[16]. However, modern biological techniques have now dramatically expanded the definition of phenotype[1]. RNA sequencing and mass spectrometry, for example, have become more widely available and less cost prohibitive, enabling the transcriptomic and proteomic characterization of individuals. Similarly, advancements in both hardware and computational tools have increased both the throughput and informational content of experiments. In this section, we examine in three specific areas the developments that have enabled deep-phenotyping studies of the worm.

Manipulating the genome. A sophisticated set of techniques, including both forward and reverse genetic approaches, can be used to manipulate the worm genome and elicit phenotypes[5]. RNAi of gene expression can be achieved by feeding worms bacteria engineered to express double-stranded RNA corresponding to a gene of interest[17,18]. This technique has enabled multiple reverse-genetic screens to identify phenotypes associated with various gene inactivations[19,20]. More recently, several research groups have introduced CRISPR-Cas9 gene editing methods optimized for manipulation of the *C. elegans* genome[21,22]. These methods allow rapid and efficient knockout of genes or introduction of fluorescent markers of gene or protein activity.

[1]School of Chemical & Biomolecular Engineering, Georgia Institute of Technology, Atlanta, GA, USA. [2]The Wallace H. Coulter Department of Biomedical Engineering, Georgia Institute of Technology and Emory University, Atlanta, GA, USA. [3]These authors contributed equally: Dhaval S. Patel and Nan Xu. *e-mail: hang.lu@gatech.edu

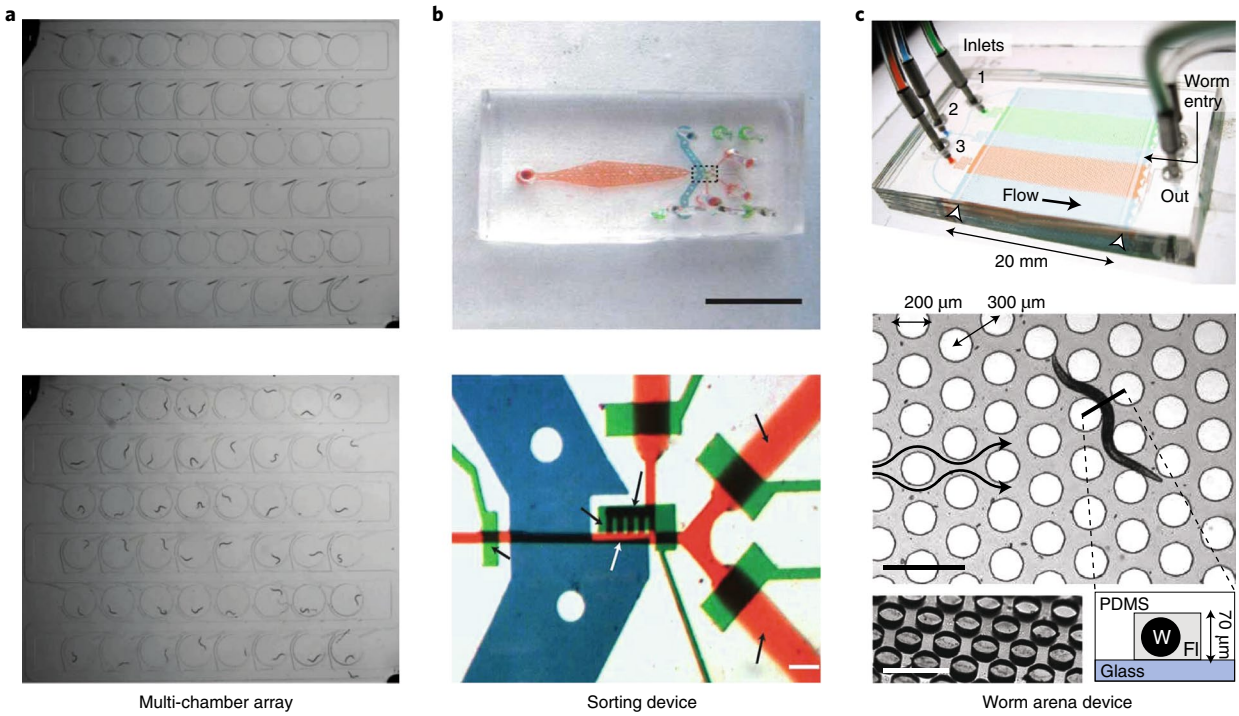

Fig. 1 | Microfluidics enables high-throughput experimentation in *C. elegans*. Examples of microfluidic devices routinely used in worm deep-phenotyping studies. **a**, Multi-chamber arrays for simultaneously studying large numbers of individual worms. **b**, Sorting devices used to rapidly isolate worms with specific characteristics. **c**, Arena devices for behavioral assays. Panel **a** adapted from ref. [29]; panel **b** adapted from ref. [24]; panel **c** adapted from ref. [28].

Hardware for deep phenotyping. Two different types of hardware development have enabled deep-phenotyping studies in worms. The first is improvement in devices for handling worms and the second is improvement in the imaging technology that records the output of an experiment. Both developments have substantially reduced component costs and produced many designs and proof-of-principle experiments, which increases the accessibility of hardware needed for deep-phenotyping experiments.

Manual handling of worms is labor intensive and limits the scale and scope of an experiment. Fortunately, the small size of the worm makes it very easy to manipulate with microfluidics[23,24]. In the past decade, microfluidic devices used by the *C. elegans* research community have been fabricated mostly from polydimethylsiloxane (PDMS). PDMS is nontoxic to worms, and fabrication of devices with this material is relatively cheap and straightforward. PDMS is also optically transparent and is therefore compatible with many types of microscopy used to study the worm. Many microfluidic devices include on-chip valves that take advantage of the elastic properties of PDMS to control the flow of fluid containing the worms. This design enables automation of animal handling and higher sample throughput[23,25–27]. In addition, microfluidics can be used to tightly control the microenvironment surrounding the worm within the device, which is hard to do on an agar plate. Device and system designs widely used for worm experiments include arena or multi-chamber arrays[28–31], imaging and sorting devices[24,27,32–37], and devices enabling more complex manipulations[38–41] (Fig. 1).

C. elegans has proven to be amenable to multiple imaging modalities. Because the worm is optically transparent, early in vivo studies of worm development used Nomarski optics to provide sufficient contrast to observe individual cell nuclei[42,43]. Various types of electron microscopy have been used for ultrastructural studies of *C. elegans*[44]. High-throughput experiments typically require the use of automated imaging systems that can quantify the intensity of fluorescent reporters. The demonstration that fluorescent protein reporters can be expressed and imaged in *C. elegans* paved the way for new types of fluorescence microscopy that are compatible with high-throughput experimentation[45]. Examples include the use of light-sheet and lattice light-sheet microscopy (LLSM) platforms to study embryogenesis[46–49] as well as protein dynamics in adult worms[50]. In the past year, a new form of LLSM with adaptive optics has been used for highly detailed imaging of cell movements during vulva development[51]. Several new microscopy platforms, including two-photon-based[52] and light-field[53,54] systems, have enabled fast volumetric whole-brain imaging of Ca^{2+} dynamics in *C. elegans*. A new form of volumetric flow cytometry using line excitation array detection has been used to monitor protein aggregation in worm models of Huntington's disease[55]. Several super-resolution microscopy systems have also been used to study embryogenesis[56,57], muscle structure[58] and the distribution of glutamate receptors[59] in *C. elegans*.

Unlike imaging techniques used to examine cellular structures or activities, many high-content behavioral studies utilize dark-field or transmission imaging to enhance the contrast of transparent worms and allow longitudinal tracking and quantification of whole-animal phenotypes[60,61]. The hardware needed for such systems is becoming cheaper and more readily available[62–65]. Behavior-tracking systems have also been integrated into microscopy systems that use targeted illumination of specific cells for optogenetic experiments in worms[66,67]. Such systems have been used to determine how the mechanosensory system of the worm encodes spatial and temporal information about stimuli to ensure appropriate behavioral responses[68,69]. The greater availability of these systems has been central to the rapid increase in behavioral deep-phenotyping studies.

Computational software for high-content phenotypic information. Due to the hardware-related gains in throughput, many experimentalists now face a dramatic increase in the amount of data produced from experiments. Making sense of these data can be beyond the analytical capability of human vision or comprehension. Therefore, extracting useful information from large volumes of data

requires workflows that can parse the content efficiently and in an interpretable manner. For image-based data, the typical structure of a deep-phenotyping workflow includes a segmentation step to identify objects of interest within each image[70,71]. This step is then followed by feature extraction and classification, which provides a quantitative breakdown of the differences between images and allows the assignment of phenotypic profiles[70,71]. Open-source image analysis platforms such as ImageJ[72,73] and CellProfiler[74], both of which have *C. elegans*-specific plugins[75–77], conveniently offer many of the computational tools required to analyze high-content data.

Several different segmentation algorithms have been applied in *C. elegans* imaging informatics. These include algorithms that segment fluorescently labeled nuclei, which have been used for cell identification and tracking during embryonic development[78–81] or within the context of a digital atlas of the L1-stage larva[82,83], as well as for tracking Ca^{2+} transients across neurons in whole-brain imaging data[84,85]. Algorithms also exist for segmenting fluorescently labeled synapses to study synaptogenesis[32,86] and for automatically tracing fluorescently labeled neurites[87] in the worm. Bright-field images can also be automatically segmented to calculate various size-related metrics of worms using the ImageJ plug-in WormSizer[88].

Machine learning is increasingly used to automate segmentation, feature extraction and classification of images in high-content workflows[70,89]. DevStaR is a machine learning-based platform that has been developed to score phenotypes automatically in worms[90]. This system can segment bright-field images and count animals belonging to different developmental stages in a mixed population. Zhan and colleagues have used a modular image-processing pipeline for the rapid development of custom supervised learning-based support-vector machines (SVM) classifiers[32,91]. This pipeline has been used to train a classifier to identify the head of the worm in bright-field images[91], as well as to train classifiers to identify neurons and differentiate between ASI and ASJ neurons[91] and between ASI, ADF and NSM neurons[92] in fluorescence microscopy images. WorMachine is another modular pipeline that can automatically score a wide range of phenotypes using trained classifiers[93]. This system can identify the sex of the animal as well as quantify complex, partially penetrant phenotypes or intracellular protein aggregation in a group of worms[93]. The development of these image analysis pipelines allows researchers without machine-vision expertise to design and perform deep-phenotyping studies in *C. elegans*. Additional examples of machine learning in imaging informatics and behavioral classification are provided below.

Applications of deep phenotyping

With the development of hardware and computational tools, deep phenotyping is now commonly used in multiple areas of worm biology. Examples of such studies are reviewed below.

Embryogenesis and lineage tracing. *C. elegans* is one of the few metazoans for which the entire somatic cell lineage can be traced from single-cell embryo to adult[42,43]. However, tracing cell lineage in the developing worm embryo is exceptionally challenging given the rapidity of cell division and morphological similarity across different cell types[94]. Because it is more complicated to identify phenotypic aberrations in the embryonic lineage than in post-embryonic cells, the mechanisms governing embryonic cell division and differentiation have been harder to elucidate. The advent of 4D imaging systems[95,96] removed the need for manual observation of embryogenesis but not for curation of the resultant images into lineages.

Deep phenotyping can be done with manually curated data. As an example, a whole-genome RNAi screen identified 661 genes involved in early embryogenesis[97], and a subsequent study integrated transcriptional, protein interaction and visual phenotypic data for these 661 genes to create predictive models of cellular events during embryogenesis[98] (Fig. 2a). The use of transgenic worms that ubiquitously express fluorescently tagged histone proteins has enabled the development of automated tracing algorithms that track embryonic lineages up to the 350-cell stage[47,79,80,99–101] (Fig. 2b).

Automated image collection and curation allows researchers to examine different aspects of embryonic cell division. Several studies have used automated lineage tracing to identify the precise cellular expression patterns of known embryonic genes[102–104]. This approach has allowed the construction of a single-cell-resolution atlas of gene expression, revealing when and where transcription factors are expressed in the developing embryo[103,104].

It is now also possible to investigate how different genetic perturbations affect embryogenesis. Early studies, for example, have identified the subtle roles of a single transcription factor[105] and the distinct roles of highly related and recently duplicated genes[106] in defining an embryonic lineage. More recent studies have demonstrated the roles of several hundred genes in cell fate choice[107,108] and in the regulation of asynchronous cell division[109]. A specific screen of chromatin regulators has also revealed distinct roles for several chromatin-modifying complexes during embryogenesis[110]. Together these studies are revealing the genetic programs and molecular mechanisms that specify how a single fertilized oocyte becomes an embryo containing a complex collection of differentiated cell types.

Whereas tools are available for deep phenotyping of embryonic development, high-throughput lineaging of post-embryonic worms has been lagging, mainly due to technical challenges imposed by the need to immobilize animals prior to imaging. However, in 2017, Keil and colleagues presented a microfluidic device that allows long-term culturing of larvae and routine immobilization of the animals, enabling high-resolution imaging with a variety of microscopy techniques[111]. Using this platform, the investigators imaged animals from the L1 larval stage through to reproductive adulthood and examined vulva precursor cell development, apoptosis during larval molting, neuron differentiation and neurite outgrowth. The emergence of new technologies such as this type of platform, coupled with future developments in post-embryonic phenotyping, is likely to lead to a complete description of the biological events involved in the development of a multicellular animal.

Automated high-throughput genetic screens. One of the most useful aspects of *C. elegans* as a model system has been that it allows forward-genetic screens to identify mutations affecting all elements of a gene, such as its promoter, exons, introns and other regulatory elements. However, most genetic screens rely on visually identifiable phenotypic differences from the control, which inherently limits the ability to identify mutations that have weak or non-obvious phenotypes but that still provide valuable information about the function of a gene. The power of deep phenotyping for identifying subtle mutants that might be missed by visual inspection has been demonstrated in automated screens to find mutations affecting synaptogenesis[32,86,112]. Using a microfluidic sorting system[32] (Fig. 1b), hundreds to thousands of worms were continuously imaged, processed and sorted in real time. An online SVM-based image-processing algorithm that had been developed to classify multidimensional features of fluorescently labeled synapses in the fly was used to process the images[32,86]. Clustering of multidimensional features for all the worms revealed the phenospace of the entire mutational spectrum[32,86] (Fig. 2c). The clusters indicate where each new mutant resides in the phenospace, allowing inference of their potential genetic relationships. This study is an example of how deep phenotyping integrates high-throughput hardware with computational tools to provide mechanistic insights that would not have been possible for a human observer.

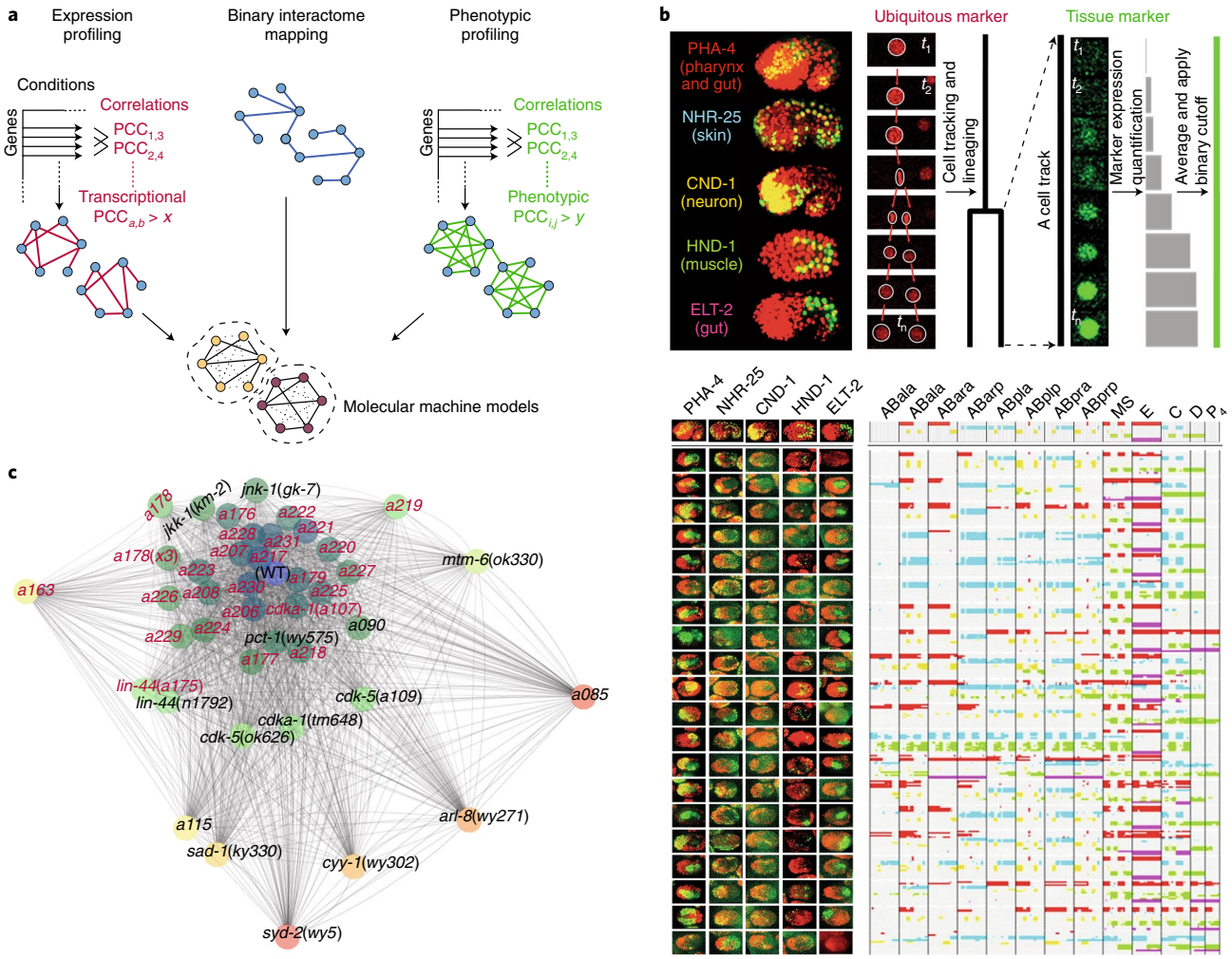

Fig. 2 | Deep phenotyping produces informationally rich datasets. a, Transcriptomic, proteomic and phenotypic data can be integrated to create models of cellular events in early embryogenesis. **b**, Use of two-color imaging can inform automated embryonic lineaging (top), which can then be used to create spatiotemporal maps of gene expression (bottom). **c**, Deep phenotyping can reveal more of the phenotypic spectrum than traditional screens. Subtle mutants (labeled in pink) lie closest to the wild type (WT), whereas previously identified mutants are farther from the WT. Panel **a** adapted from ref. [98]; panel **b** adapted from ref. [108]; panel **c** adapted from ref. [86].

Measuring aging and age-related decline. Over the past 30 years, scientists have made a concerted effort to understand the biology of aging. *C. elegans* is the premier model organism for the study of longevity because of its short lifespan and powerful genetics[113]. The majority of lifespan studies in worms are performed manually; animals maintained on agar plates are periodically examined under a stereomicroscope for either spontaneous or stimulated movement[114]. These manual experiments constrain the types of phenotypic data and the scale of demographic data that a human observer can obtain. Deep-phenotyping technologies offer more efficient and cost-effective collection of high-throughput and high-temporal-resolution lifespan data.

The first automated aging studies in worms used scanners to capture time-lapse data showing worm movement on agar plates[115,116]. In these systems, death is defined as a persistent absence of movement, as the worms cannot be stimulated to test for induced movement. Stroustrup and colleagues have used their automated system, termed the lifespan machine[116], to examine the demographic features of large populations[117]. At the population level, in groups that had very different lifespans after exposure to factors such as changes in ambient temperature or chemically induced stress, aging appeared to scale temporally; plots of survival against time for worms in different conditions could be superimposed by rescaling the time axis. This scaling implies that a single effective constant rate governs aging in *C. elegans* and that interventions that altered longevity did so by changing this rate[117].

These scanner-based lifespan studies cannot gather data at the level of the individual because their temporal resolution does not allow tracking of each worm until it dies[116]. As a result, these systems cannot assess inter-individual variation in lifespan within a population, which can be large even for isogenic worms raised in identical conditions[118]. In the past 3 years, two groups have achieved robust high-throughput automated acquisition of lifespan data from individual animals[30,31,119]. Pittman and colleagues used a polyethylene glycol (PEG) hydrogel substrate seeded with spots of *Escherichia coli* as a food source for developing *C. elegans* embryos, each of which is individually placed in a single spot; once the embryos are deposited, the substrate is sealed using a layer of PDMS[31]. The PDMS acts as a barrier confining each animal upon hatching to its local spot of *E. coli*. The PEG substrate can then be imaged using a wide array of microscopy platforms, allowing researchers to track multiple features of the development and lifespan of each worm individually. Zhang and colleagues have used this system to show that when tracked at the level of the individual, aging does not display

temporal scaling, with long-lived animals showing an extended decrepitude phase—termed twilight—compared with short-lived individuals[119]. The WorMotel platform[30,62] can record both spontaneous and stimulated movement; stimulated movement is evoked by a brief pulse of blue light to assess whether a worm is alive or not. Using this system, Churgin and colleagues have also demonstrated that short-lived and long-lived individual lifespans from an isogenic population do not temporally scale[30]. The differences seen between population-level measures of longevity and measures that account for inter-individual variability demonstrate the increasing power of deep-phenotyping technologies to study biological processes.

Dietary restriction (DR) has been shown to extend robustly lifespan in an evolutionarily conserved manner[120]. There is considerable interest, from researchers in both academia and the pharmaceutical industry, in finding drugs that can induce the phenotypic effects of DR in humans without the concomitant need for drastic diet change. Using the lifespan machine[116], Lucanic and colleagues designed a high-throughput screen to identify potential DR mimetics in *C. elegans*[121]. The investigators screened a library of 30,000 small molecules, identifying 57 compounds that repeatedly extended the lifespan of treated animals compared with control worms. Several of these compounds were structurally related and contained a nitrophenyl piperazine moiety; further analysis of the most effective of the nitrophenyl piperazine compounds, NP1, suggested that it extended longevity by inducing DR-like effects[121].

One of the reasons for the rising interest in the study of aging is that the incidence of both cognitive impairment and neurodegenerative disease increases with old age, which imposes a substantial societal cost as the proportion of elderly individuals relative to those of working age continues to grow in the general population[122]. The research community seeks to develop treatments that can counteract the debilitating neurological effects of aging. *C. elegans* also displays age-related declines in cognitive ability and in the morphological structure of its nervous system[123]. Bazopoulou and colleagues have developed a microfluidic platform to monitor the Ca^{2+} responses of a specific polymodal neuron, ASH, as it ages[124]. They used this system to conduct a pilot screen to identify small molecules that could delay the age-related decline of ASH activity. Several molecules from a panel of 107 FDA-approved compounds delayed the decline of Ca^{2+} responses in ASH during aging; the most effective of these compounds were tiagabine and honokiol[124]. This study demonstrates that deep-phenotyping technologies can acquire dynamic readouts, such as neural activity, in a high-content manner.

Drug discovery and small-molecule biology. Deep phenotyping is increasingly being embraced by researchers in the field of drug discovery because it allows rapid screening of the pleiotropic effects of different molecules. Due to its ease of culture and amenability to high-throughput experimentation, the worm has been used to model many different human diseases[125,126]. Although many researchers are developing methodologies to speed up drug discovery using worm models of disease, these platforms do not fit our definition of deep phenotyping as they tend to analyze single and relatively simple phenotypes. However, we review these methodologies here because they may suggest how newer deep-phenotyping platforms will transform drug discovery screens in model organisms.

The phenotype of diseased hepatocytes has been replicated in a worm model of cirrhosis expressing a mutant human α1-antitrypsin (ATZ) fused to green fluorescent protein (GFP) that aggregates within the endoplasmic reticulum of intestinal cells[126]. A plate reader-based screen of a commercially available compound library yielded 33 compounds that decreased the rate of GFP aggregation within this worm's intestinal cells[126]. More recently, a high-throughput genome-scale RNAi screen of ATZ model worms was performed to find gene inactivations that alter intestinal GFP aggregation; the study identified 100 genes whose inactivation decreased GFP aggregation in the ATZ worms. Using an in silico approach, the investigators identified drugs known to target the mammalian orthologs of the worm genes and tested them for rescue of the GFP-aggregation phenotype[127].

Polyglutamine expansion (polyQ) diseases, such as Huntington's disease, are another example of protein-aggregation disorders that have been modeled successfully in worms[128]. A 2016 study unveiled a high-resolution microfluidic system for high-throughput drug discovery using a worm polyQ model as a demonstration of the platform's potential[129]. With this platform, Mondal and colleagues rapidly screened around 100,000 worms to test 983 FDA-approved compounds for their ability to reduce yellow fluorescent protein (YFP) aggregation in a high-polyQ strain[129]. The screen identified four compounds that induced a significant reduction in protein aggregation. Another high-resolution microfluidic system has been developed to identify compounds that affect axon regeneration in *C. elegans*[130]. This platform was used to perform high-throughput laser microsurgery specifically on the axons of the PLM neuron and then move the axotomized worms into media containing different compounds to test the effects on neurite regrowth. This screen revealed that the compounds staurosporine and prostratin could, respectively, inhibit and promote axonal regeneration[130].

The use of deep-phenotyping technologies might also enable cost-effective studies of widespread but often neglected diseases. Parasitic nematodes, for example, are thought to infect a billion people worldwide and are also a substantial source of infection in many animals and plants that humans depend on for their food and livelihoods. However, the development of anthelmintic drugs has not kept pace with the acquisition of drug resistance by these nematodes, and therefore new therapeutics are urgently needed[131,132]. Since parasitic nematodes are difficult to work with directly because they need to grow in a host system, *C. elegans* has become a model system for anthelmintic toxicology. The WormScan platform can simultaneously measure the mobility, brood size, body size and lifespan of worms either on agar plates or in liquid culture[115,131]. This system was used to screen 26,000 compounds, resulting in the identification of 14 potential anthelmintic compounds. The Invertebrate Automated Phenotyping Platform (INVAPP) also utilizes a 96-well-plate format for culturing worms in liquid. However, the automated image capture relies on a high-frame-rate camera instead of a scanner, giving this system increased sensitivity in the detection of drug-induced motility defects[132]. A proof-of-concept drug screen using INVAPP with a 400-compound library identified 14 molecules that impaired worm growth[132]. A separate compound-library screen against the parasitic nematode *Trichuris muris* using the INVAPP platform and the Paragon algorithm uncovered an entirely new class of promising anthelmintics[133]. Such deep-phenotyping studies of *C. elegans* allow researchers to rapidly identify potential anthelminthic drugs and their modes of action without performing the complex in-host assays required to study parasitic worms.

Small-molecule screens are not only a tool to identify therapeutic chemicals; they can also be used to study the biology of genetic pathways. The gene *skn-1* encodes a transcription factor that regulates the worm's response to oxidative and xenobiotic stress[134]. Leung and colleagues performed a plate reader-based screen for small-molecule activators of the protein skinhead-1 (SKN-1) by measuring the induction of a GFP-based transcriptional reporter of the *skn-1* target gene *gst-4*[135]. The investigators then performed an ultra-high-throughput screen for inhibitors of SKN-1 in a compound library containing >364,000 small molecules[136]. This screen identified 125 molecules that specifically lowered the fluorescence signal of the *gst-4::gfp* reporter compared with a control, suggesting that these molecules are SKN-1 inhibitors[136]. A similar strategy was used to study the male-specific linker cell, which undergoes cell death just after the molt between the fourth larval stage and

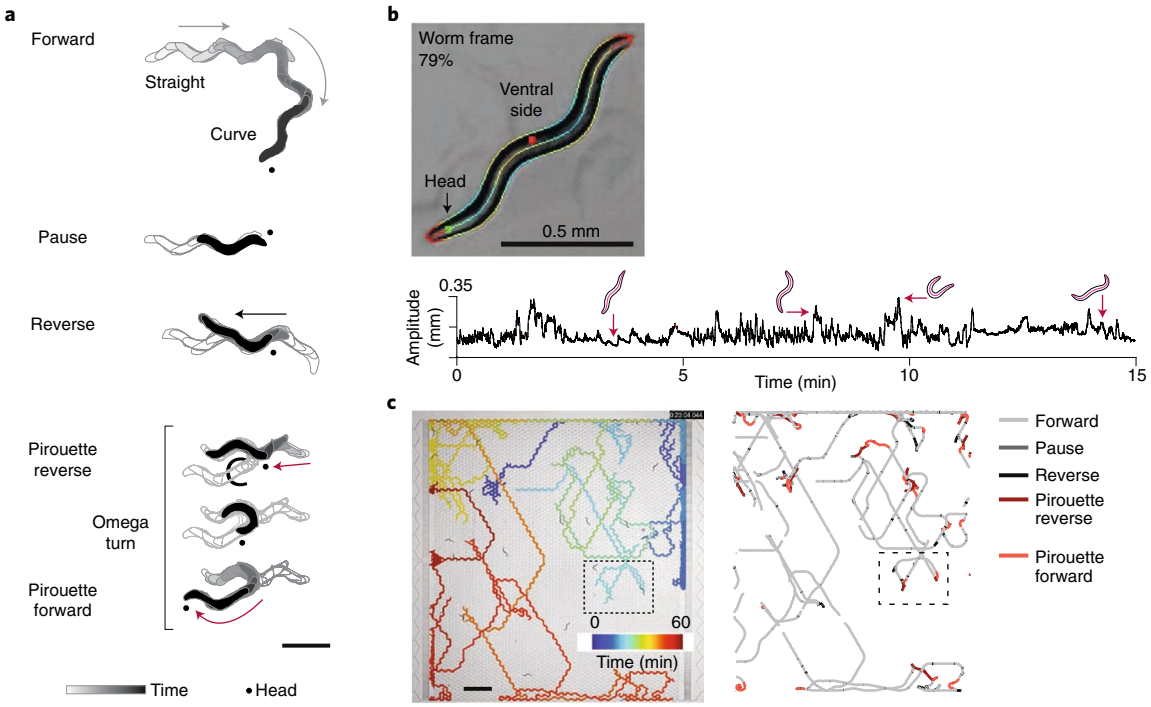

Fig. 3 | Behavioral deep phenotyping of worms using automated trackers. a, Behavioral repertoire of *C. elegans* that can be automatically tracked. **b**, Example of a single worm's behavior during an experiment. **c**, A multi-worm tracking system developed for tracking behaviors in a group of worms. Panels **a**,**c** adapted from ref. [28]; panel **b** adapted from ref. [141].

adulthood[137]. The death of this cell is independent of caspases, therefore non-apoptotic, and shares many morphological features with other non-apoptotic cell death observed in vertebrate development[137]. Schwendeman and Shaham performed a proof-of-concept small-molecule screen to identify potential inhibitors of linker-cell death that might shed further light on the biology of this phenomenon[138]. A screen of 23,797 compounds using a laser-scanning cytometer identified six compounds that caused persistence of the linker cell by inducing some form of global developmental delay in the worms that was rescuable upon removal of the worms from the drug[138]. Together these studies demonstrate how the use of deep-phenotyping technologies might enable quantitative measurement of multiple morphometric traits to gain new insight into biology.

Behavioral analyses of freely moving worms. One of the original motivations that drove the development of *C. elegans* as a model system was the desire to understand how the nervous system of an animal gives rise to its behaviors[16]. The history and biological significance of behavioral studies of *C. elegans* were extensively reviewed by McDiarmid and colleagues in 2017[61]. In this Review, we briefly discuss improvements in worm-tracking hardware and software in the past 20 years and show how deep-phenotyping studies might reveal mechanisms underlying emergent behaviors.

The rapidity of behavior changes in freely moving worms makes it nearly impossible for a human observer to record all events in real time. Therefore, the majority of behavioral studies use some form of automated imaging. The earliest tracking systems could record the spatial position, speed and turning rate of individual worms[139]. Newer tracking platforms offer more comprehensive descriptions of worm behavior. Worm-tracking systems fall into two categories: single-worm trackers for high-resolution analysis of individual behavior[140–143] and multi-worm systems for population-level studies[65,144–149] (Fig. 3). These systems have elucidated the behavioral genetics of several sensory modalities. Explicit analyses of different behavioral features of thousands of animals from 239 genotypes uncovered 87 genes involved in locomotion, including components of the Gαq signaling pathway, and predicted 370 specific genetic interactions among them[150]. Similar studies have identified genes involved in thermotaxis[151], chemotaxis[144,152] and mechanosensation[144]. Most of these studies were performed on agar plates. However, the development of microfluidic arenas now allows for precise spatiotemporal control of the chemical environment, revealing behaviors that are not observable in plate-based experiments[28].

In addition to the improvements in worm-tracker hardware, the development of new algorithms has led to a more comprehensive description of worm behaviors. For example, principal component analysis has been used to decompose the postural space of worms into eigenvectors referred to as eigenworms[153]. Surprisingly, the study showed that the postural space of locomoting worms on agar plates is low dimensional and that the superposition of just four eigenworms is sufficient to describe the majority of the worm's locomotory postures. This analysis, which dramatically reduces the complexity of quantifying behavioral patterns, has been built into many worm-tracking systems[141,144,153,154]. The approach has enabled deep-phenotyping studies of behavioral dynamics, such as the creation of a dictionary of behavioral motifs curated from both wild-type and 307 mutant strains[154]. Similarly, an extensive phenotypic database of locomotory behaviors for a large number of strains was compiled through comprehensive behavioral recording for multiple alleles of the same gene as well as some double and triple mutants[141]. These dictionaries[154] and databases[141] uncover subtle behavioral phenotypes that cannot be discerned by manual observation, underscoring the importance of deep-phenotyping pipelines.

There is still limited understanding of how behaviors emerge from the integration of information from the external environment and the worm's internal state. This problem has been studied extensively in food-related behaviors[155]. The behavioral state transitions that a worm undergoes while foraging, as well as the informational value of the food it encounters, can be modeled mathematically[156–158], and these models can be used to predict the

worm's response to food[156,158]. We anticipate that the integration of such predictive models into deep-phenotyping studies will lead to greater mechanistic insight into the genetics of foraging behavior. Increasing experimental throughput is also essential to achieve deep phenotyping of foraging behavior. WorMotel allows for highly parallelized monitoring of individual worms under uniformly controlled environmental conditions[30,62]. This platform has been used to examine the relationship between food abundance and roaming (active) or dwelling (sedentary) behaviors[159,160]. These studies reveal the biological complexity of foraging behaviors. For example, serotonin produced by ADF neurons promotes roaming, whereas serotonin produced by NSM neurons promotes dwelling[160]. Other biological amines such as dopamine promote dwelling[159], whereas octopamine is involved in roaming behaviors[160].

Similar experimental parallelization has been performed in plate-based foraging assays with the use of multiple cheap cameras[161]. Stern and colleagues examined roaming and dwelling behaviors in individual worms continuously across their development[161]. The pattern of behaviors varied reproducibly across different developmental stages as well as between the onset and exit phases of each larval stage. The study showed that a suite of neuromodulators is responsible for the regulation of these behavioral patterns[161]. Interestingly, by tracking individual worms throughout their development, the investigators also identified striking inter-individual variation in roaming behavior. Even though the worms were derived from isogenic populations, some animals consistently roamed less across all developmental stages, whereas others consistently roamed more[161]. Quantifying this type of stochastic variation in any phenotype and understanding its biological origins is challenging given the large numbers of individuals that must be surveyed. Deep phenotyping offers a way to integrate high-throughput experimentation with comprehensive behavioral analysis.

Whole-brain imaging: the next frontier in deep phenotyping. How the nervous system encodes external environmental information to modulate animal behavior is the subject of intense examination in biology. This question becomes even more challenging to answer in natural habitats, where the environment contains a myriad of conflicting cues that an animal must successfully integrate to perform behaviors that maximize its chance of survival. In *C. elegans*, the nervous system is essentially divided into three layers: sensory neurons that detect external stimuli, interneurons that integrate information from sensory neurons, and motor neurons that control the behavior of the worm, with a few polymodal neurons that perform several of these functions[162]. It is a complex problem to understand how the different layers receive and process information and communicate with one another to ensure the appropriate outcome. For example, the aversive chemotactic response to isoamyl alcohol exposure is stochastic, even though the chemosensory neuron that detects the stimulant depolarizes in a deterministic way[163]. The behavioral stochasticity of this chemotaxis circuit is generated at the level of interneurons via their collective activity[163]. The development of genetically encoded Ca^{2+} indicators has allowed imaging of neuronal activity in the worm, ranging from a single neuron all the way up to the entire brain[164]. This development, in turn, has paved the way for whole-brain imaging platforms for long-term observation and analysis of large numbers of neurons. The goal of these systems is to dissect neuronal activity and identify not only neural circuits associated with specific behaviors, but also global states that reflect the functional architecture of the brain.

Several studies have successfully characterized whole-brain dynamics under various experimental conditions. Kato and colleagues used a microfluidic imaging platform to carry out whole-brain recordings from immobilized worms, which revealed that the time evolution of network dynamics among neurons is directional and cyclical[165]. Different phases in this cyclical activity regulate motor commands that drive certain locomotory behaviors. Using a spinning-disk confocal system, Venkatachalam and colleagues developed a whole-brain imaging platform and studied representations of sensory input and motor output of individual neurons upon thermosensory stimulus in freely moving worms[166]. Similarly, using a simultaneous worm-tracking and whole-brain imaging system, Nguyen and colleagues recorded whole-brain activity of freely moving worms without stimulation[85,167]; in a related effort, Nguyen and colleagues used machine learning to track neurons in the freely moving heads of worms, which is an important step toward robustly and automatically analyzing such large sets of dynamical data[85]. More recently, Nichols and colleagues investigated global brain dynamics during lethargus, a sleep-like state in the worm[168]. The study showed that global brain activity becomes quiescent during lethargus; however, specific neurons remain active as these cells promote the establishment of the quiescence. By examining whole-brain dynamics, this work demonstrated that the transition to the wakeful state is carried out via reestablishment of activity in specific neurons that drives global brain dynamics back to the aroused state[168].

The examples reviewed above show the benefit of studying the entire nervous system rather than analyzing specific subsets of neurons, given that researchers have not identified all the neurons or functional connections in circuits governing various sensorimotor behaviors. These examples also point to opportunities for future technological and theoretical developments in analyzing and understanding such complex and dynamical systems. For instance, the field still needs better imaging systems that allow coupling of other experimental techniques such as optogenetics. Automatic identification of neurons is also needed, along with new tracking algorithms that are more accurate, faster or both. Furthermore, better theories might be needed in the future for interpreting large volumes of curated data and making sense of how the brain processes information and makes decisions.

Future outlook

In this Review, we have highlighted many recent conceptual and methodological developments for deep phenotyping using *C. elegans* as a model system. The success of these studies clearly indicates that by measuring many aspects of the morphology, functional output and behavior of cells, as well as circuits, tissues and individual animals, we can expand the scope of biological studies. Furthermore, by using appropriate mathematical and statistical tools, we can better understand the mechanisms underlying many biological processes. We believe that these approaches will become more ubiquitous as improved microscopy and other experimental tools as well as analytical pipelines using advanced computational and theoretical techniques become more accessible.

Although many of the tools discussed above were used in a *C. elegans*-specific context, they are applicable to a broad range of biological systems. For example, microfluidics is widely used in the analysis of single cells, with platforms such as DropMap providing high-content, single-cell-resolution analysis of IgG-secreting cells[169]. Substantial progress has also been made in developing automated animal handling and tracking systems that can work with diverse organisms. The MAPLE robotic system and its derivatives can perform deep-phenotyping experiments on *Saccharomyces cerevisiae*, *Physarum polycephalum*, *Bombus impatiens* and *Drosophila melanogaster* in addition to *C. elegans*[65,170]. Several studies have also demonstrated the feasibility of deep phenotyping in the vertebrate model system *Danio rerio*. High-throughput optical-projection tomography has been used to measure gene expression changes across the brains of different mutants of zebrafish[171]. Similarly, micron-scale tomography[172] has been used to study the determinants of skeletal development in zebrafish[173]. We predict that the future integration of efforts in different disciplines such as biology, engineering and computational sciences will considerably accelerate progress in linking phenotypes to genotypes, environmental conditions and stochasticity.

Received: 26 September 2018; Accepted: 17 May 2019;
Published online: 19 June 2019

References

1. Houle, D., Govindaraju, D. R. & Omholt, S. Phenomics: the next challenge. *Nat. Rev. Genet.* **11**, 855–866 (2010).
2. Raj, A. & van Oudenaarden, A. Nature, nurture, or chance: stochastic gene expression and its consequences. *Cell* **135**, 216–226 (2008).
3. Honegger, K. & de Bivort, B. Stochasticity, individuality and behavior. *Curr. Biol.* **28**, R8–R12 (2018).
4. Tracy, R. P. 'Deep phenotyping': characterizing populations in the era of genomics and systems biology. *Curr. Opin. Lipidol.* **19**, 151–157 (2008).
5. Corsi, A. K., Wightman, B. & Chalfie, M. A transparent window into biology: a primer on *Caenorhabditis elegans*. *Genetics* **200**, 387–407 (2015).
6. Shaye, D. D. & Greenwald, I. OrthoList: a compendium of *C. elegans* genes with human orthologs. *PLoS One* **6**, e20085 (2011).
7. Ellis, H. M. & Horvitz, H. R. Genetic control of programmed cell death in the nematode *C. elegans*. *Cell* **44**, 817–829 (1986).
8. Hedgecock, E. M., Culotti, J. G. & Hall, D. H. The *unc-5*, *unc-6*, and *unc-40* genes guide circumferential migrations of pioneer axons and mesodermal cells on the epidermis in *C. elegans*. *Neuron* **4**, 61–85 (1990).
9. Ishii, N., Wadsworth, W. G., Stern, B. D., Culotti, J. G. & Hedgecock, E. M. UNC-6, a laminin-related protein, guides cell and pioneer axon migrations in *C. elegans*. *Neuron* **9**, 873–881 (1992).
10. Lee, R. C., Feinbaum, R. L. & Ambros, V. The *C. elegans* heterochronic gene *lin-4* encodes small RNAs with antisense complementarity to *lin-14*. *Cell* **75**, 843–854 (1993).
11. Wightman, B., Ha, I. & Ruvkun, G. Posttranscriptional regulation of the heterochronic gene *lin-14* by *lin-4* mediates temporal pattern formation in *C. elegans*. *Cell* **75**, 855–862 (1993).
12. Fire, A. et al. Potent and specific genetic interference by double-stranded RNA in *Caenorhabditis elegans*. *Nature* **391**, 806–811 (1998).
13. Fadeel, B. & Orrenius, S. Apoptosis: a basic biological phenomenon with wide-ranging implications in human disease. *J. Intern. Med.* **258**, 479–517 (2005).
14. Lekka, E. & Hall, J. Noncoding RNAs in disease. *FEBS Lett.* **592**, 2884–2900 (2018).
15. Van Battum, E. Y., Brignani, S. & Pasterkamp, R. J. Axon guidance proteins in neurological disorders. *Lancet Neurol.* **14**, 532–546 (2015).
16. Brenner, S. The genetics of *Caenorhabditis elegans*. *Genetics* **77**, 71–94 (1974).
17. Timmons, L., Court, D. L. & Fire, A. Ingestion of bacterially expressed dsRNAs can produce specific and potent genetic interference in *Caenorhabditis elegans*. *Gene* **263**, 103–112 (2001).
18. Timmons, L. & Fire, A. Specific interference by ingested dsRNA. *Nature* **395**, 854 (1998).
19. Kamath, R. S. et al. Systematic functional analysis of the *Caenorhabditis elegans* genome using RNAi. *Nature* **421**, 231–237 (2003).
20. Rual, J. F. et al. Toward improving *Caenorhabditis elegans* phenome mapping with an ORFeome-based RNAi library. *Genome Res.* **14**, 2162–2168 (2004).
21. Dickinson, D. J. & Goldstein, B. CRISPR-based methods for *Caenorhabditis elegans* genome engineering. *Genetics* **202**, 885–901 (2016).
22. Farboud, B. Targeted genome editing in *Caenorhabditis elegans* using CRISPR/Cas9. *Wiley Interdiscip. Rev. Dev. Biol.* **6**, e287 (2017).
23. Crane, M. M., Chung, K., Stirman, J. & Lu, H. Microfluidics-enabled phenotyping, imaging, and screening of multicellular organisms. *Lab. Chip* **10**, 1509–1517 (2010).
24. Chung, K., Crane, M. M. & Lu, H. Automated on-chip rapid microscopy, phenotyping and sorting of *C. elegans*. *Nat. Methods* **5**, 637–643 (2008).
25. Ben-Yakar, A., Chronis, N. & Lu, H. Microfluidics for the analysis of behavior, nerve regeneration, and neural cell biology in *C. elegans*. *Curr. Opin. Neurobiol* **19**, 561–567 (2009).
26. Cornaglia, M., Lehnert, T. & Gijs, M. A. M. Microfluidic systems for high-throughput and high-content screening using the nematode *Caenorhabditis elegans*. *Lab. Chip* **17**, 3736–3759 (2017).
27. Lee, H. et al. A multi-channel device for high-density target-selective stimulation and long-term monitoring of cells and subcellular features in *C. elegans*. *Lab. Chip* **14**, 4513–4522 (2014).
28. Albrecht, D. R. & Bargmann, C. I. High-content behavioral analysis of *Caenorhabditis elegans* in precise spatiotemporal chemical environments. *Nat. Methods* **8**, 599–605 (2011).
29. Chung, K. et al. Microfluidic chamber arrays for whole-organism behavior-based chemical screening. *Lab. Chip* **11**, 3689–3697 (2011).
30. Churgin, M. A. et al. Longitudinal imaging of *Caenorhabditis elegans* in a microfabricated device reveals variation in behavioral decline during aging. *Elife* **6**, e26652 (2017).
31. Pittman, W. E., Sinha, D. B., Zhang, W. B., Kinser, H. E. & Pincus, Z. A simple culture system for long-term imaging of individual *C. elegans*. *Lab. Chip* **17**, 3909–3920 (2017).
32. Crane, M. M. et al. Autonomous screening of *C. elegans* identifies genes implicated in synaptogenesis. *Nat. Methods* **9**, 977–980 (2012).
33. Krajniak, J., Hao, Y., Mak, H. Y. & Lu, H. C.L.I.P.—continuous live imaging platform for direct observation of *C. elegans* physiological processes. *Lab. Chip* **13**, 2963–2971 (2013).
34. Kopito, R. B. & Levine, E. Durable spatiotemporal surveillance of *Caenorhabditis elegans* response to environmental cues. *Lab. Chip* **14**, 764–770 (2014).
35. Gokce, S. K. et al. A multi-trap microfluidic chip enabling longitudinal studies of nerve regeneration in *Caenorhabditis elegans*. *Sci. Rep.* **7**, 9837 (2017).
36. Rouse, T., Aubry, G., Cho, Y., Zimmer, M. & Lu, H. A programmable platform for sub-second multichemical dynamic stimulation and neuronal functional imaging in *C. elegans*. *Lab. Chip* **18**, 505–513 (2018).
37. Casadevall i Solvas, X. et al. High-throughput age synchronisation of *Caenorhabditis elegans*. *Chem. Commun. (Camb)* **47**, 9801–9803 (2011).
38. Cho, Y., Oakland, D. N., Lee, S. A., Schafer, W. R. & Lu, H. On-chip functional neuroimaging with mechanical stimulation in *Caenorhabditis elegans* larvae for studying development and neural circuits. *Lab. Chip* **18**, 601–609 (2018).
39. Cho, Y. et al. Automated and controlled mechanical stimulation and functional imaging in vivo in *C. elegans*. *Lab. Chip* **17**, 2609–2618 (2017).
40. Rahman, M. et al. NemaFlex: a microfluidics-based technology for standardized measurement of muscular strength of *C. elegans*. *Lab. Chip* **18**, 2187–2201 (2018).
41. Lockery, S. R. et al. A microfluidic device for whole-animal drug screening using electrophysiological measures in the nematode *C. elegans*. *Lab. Chip* **12**, 2211–2220 (2012).
42. Sulston, J. E. & Horvitz, H. R. Post-embryonic cell lineages of the nematode, *Caenorhabditis elegans*. *Dev. Biol.* **56**, 110–156 (1977).
43. Sulston, J. E., Schierenberg, E., White, J. G. & Thomson, J. N. The embryonic cell lineage of the nematode *Caenorhabditis elegans*. *Dev. Biol.* **100**, 64–119 (1983).
44. Hall, D. H., Hartwieg, E. & Nguyen, K. C. Modern electron microscopy methods for *C. elegans*. *Methods Cell. Biol.* **107**, 93–149 (2012).
45. Chalfie, M., Tu, Y., Euskirchen, G., Ward, W. W. & Prasher, D. C. Green fluorescent protein as a marker for gene expression. *Science* **263**, 802–805 (1994).
46. Chen, B. C. et al. Lattice light-sheet microscopy: imaging molecules to embryos at high spatiotemporal resolution. *Science* **346**, 1257998 (2014).
47. Mace, D. L., Weisdepp, P., Gevirtzman, L., Boyle, T. & Waterston, R. H. A. High-fidelity cell lineage tracing method for obtaining systematic spatiotemporal gene expression patterns in *Caenorhabditis elegans*. *G3 (Bethesda)* **3**, 851–863 (2013).
48. Wu, Y. et al. Inverted selective plane illumination microscopy (iSPIM) enables coupled cell identity lineaging and neurodevelopmental imaging in *Caenorhabditis elegans*. *Proc. Natl Acad. Sci. U S A* **108**, 17708–17713 (2011).
49. Wu, Y. et al. Spatially isotropic four-dimensional imaging with dual-view plane illumination microscopy. *Nat. Biotechnol.* **31**, 1032–1038 (2013).
50. Rieckher, M. et al. A customized light sheet microscope to measure spatio-temporal protein dynamics in small model organisms. *PLoS One* **10**, e0127869 (2015).
51. Liu, T. L. et al. Observing the cell in its native state: Imaging subcellular dynamics in multicellular organisms. *Science* **360**, eaaq1392 (2018).
52. Schrodel, T., Prevedel, R., Aumayr, K., Zimmer, M. & Vaziri, A. Brain-wide 3D imaging of neuronal activity in *Caenorhabditis elegans* with sculpted light. *Nat. Methods* **10**, 1013–1020 (2013).
53. Prevedel, R. et al. Simultaneous whole-animal 3D imaging of neuronal activity using light-field microscopy. *Nat. Methods* **11**, 727–730 (2014).
54. Shaw, M., Elmi, M., Pawar, V. & Srinivasan, M. A. Investigation of mechanosensation in *C. elegans* using light field calcium imaging. *Biomed. Opt. Express* **7**, 2877–2887 (2016).
55. Martin, C. et al. Line excitation array detection fluorescence microscopy at 0.8 million frames per second. *Nat. Commun.* **9**, 4499 (2018).
56. Gao, L. et al. Noninvasive imaging beyond the diffraction limit of 3D dynamics in thickly fluorescent specimens. *Cell* **151**, 1370–1385 (2012).
57. Ingaramo, M. et al. Two-photon excitation improves multifocal structured illumination microscopy in thick scattering tissue. *Proc. Natl Acad. Sci. U S A* **111**, 5254–5259 (2014).
58. Qadota, H. et al. High-resolution imaging of muscle attachment structures in *Caenorhabditis elegans*. *Cytoskeleton (Hoboken)* **74**, 426–442 (2017).
59. Vangindertael, J. et al. Super-resolution mapping of glutamate receptors in *C. elegans* by confocal correlated PALM. *Sci. Rep.* **5**, 13532 (2015).
60. Husson, S.J., Costa, W.S., Schmitt, C. & Gottschalk, A. Keeping track of worm trackers. *WormBook* https://doi.org/10.1895/wormbook.1.156.1 (2013).
61. McDiarmid, T. A., Yu, A. J. & Rankin, C. H. Beyond the response—high throughput behavioral analyses to link genome to phenome in *Caenorhabditis elegans*. *Genes Brain Behav.* **17**, e12437 (2018).

62. Churgin, M. A. & Fang-Yen, C. An imaging system for *C. elegans* behavior. *Methods Mol. Biol.* **1327**, 199–207 (2015).
63. Liu, Z., Tian, L., Liu, S. & Waller, L. Real-time brightfield, darkfield, and phase contrast imaging in a light-emitting diode array microscope. *J. Biomed. Opt.* **19**, 106002 (2014).
64. Yu, C. C., Raizen, D. M. & Fang-Yen, C. Multi-well imaging of development and behavior in *Caenorhabditis elegans*. *J. Neurosci. Methods* **223**, 35–39 (2014).
65. Alisch, T., Crall, J. D., Kao, A. B., Zucker, D. & de Bivort, B. L. MAPLE (modular automated platform for large-scale experiments), a robot for integrated organism-handling and phenotyping. *Elife* **7**, e37166 (2018).
66. Leifer, A. M., Fang-Yen, C., Gershow, M., Alkema, M. J. & Samuel, A. D. Optogenetic manipulation of neural activity in freely moving *Caenorhabditis elegans*. *Nat. Methods* **8**, 147–152 (2011).
67. Stirman, J. N. et al. Real-time multimodal optical control of neurons and muscles in freely behaving *Caenorhabditis elegans*. *Nat. Methods* **8**, 153–158 (2011).
68. Liu, M., Sharma, A. K., Shaevitz, J. W. & Leifer, A. M. Temporal processing and context dependency in *Caenorhabditis elegans* response to mechanosensation. *Elife* **7**, e36419 (2018).
69. Porto, D. A., Giblin, J., Zhao, Y. & Lu, H. Reverse-correlation analysis of the mechanosensation circuit and behavior in *C. elegans* reveals temporal and spatial encoding. *Sci. Rep.* **9**, 5182 (2019).
70. Grys, B. T. et al. Machine learning and computer vision approaches for phenotypic profiling. *J. Cell Biol.* **216**, 65–71 (2017).
71. Wollmann, T., Erfle, H., Eils, R., Rohr, K. & Gunkel, M. Workflows for microscopy image analysis and cellular phenotyping. *J. Biotechnol.* **261**, 70–75 (2017).
72. Rueden, C. T. et al. ImageJ2: ImageJ for the next generation of scientific image data. *BMC Bioinformatics* **18**, 529 (2017).
73. Schindelin, J. et al. Fiji: an open-source platform for biological-image analysis. *Nat. Methods* **9**, 676–682 (2012).
74. McQuin, C. et al. CellProfiler 3.0: next-generation image processing for biology. *PLoS Biol.* **16**, e2005970 (2018).
75. Wahlby, C. et al. An image analysis toolbox for high-throughput *C. elegans* assays. *Nat. Methods* **9**, 714–716 (2012).
76. Jung, S. K., Aleman-Meza, B., Riepe, C. & Zhong, W. QuantWorm: a comprehensive software package for *Caenorhabditis elegans* phenotypic assays. *PLoS One* **9**, e84830 (2014).
77. Labocha, M. K., Jung, S. K., Aleman-Meza, B., Liu, Z. & Zhong, W. WormGender—Open-source software for automatic *Caenorhabditis elegans* sex ratio measurement. *PLoS One* **10**, e0139724 (2015).
78. Chen, L., Chan, L. L., Zhao, Z. & Yan, H. A novel cell nuclei segmentation method for 3D *C. elegans* embryonic time-lapse images. *BMC Bioinformatics* **14**, 328 (2013).
79. Santella, A., Du, Z., Nowotschin, S., Hadjantonakis, A. K. & Bao, Z. A hybrid blob-slice model for accurate and efficient detection of fluorescence labeled nuclei in 3D. *BMC Bioinformatics* **11**, 580 (2010).
80. Santella, A., Du, Z. & Bao, Z. A semi-local neighborhood-based framework for probabilistic cell lineage tracing. *BMC Bioinformatics* **15**, 217 (2014).
81. Zichuan, L. et al. NucleiNet: A convolutional encoder-decoder network for bio-image denoising. *Conf. Proc. IEEE Eng. Med. Biol. Soc.* **2017**, 1986–1989 (2017).
82. Long, F., Peng, H., Liu, X., Kim, S. K. & Myers, E. A 3D digital atlas of *C. elegans* and its application to single-cell analyses. *Nat. Methods* **6**, 667–672 (2009).
83. Qu, L. et al. Simultaneous recognition and segmentation of cells: application in *C. elegans*. *Bioinformatics* **27**, 2895–2902 (2011).
84. Toyoshima, Y. et al. Accurate automatic detection of densely distributed cell nuclei in 3D space. *PLoS Comput. Biol.* **12**, e1004970 (2016).
85. Nguyen, J. P., Linder, A. N., Plummer, G. S., Shaevitz, J. W. & Leifer, A. M. Automatically tracking neurons in a moving and deforming brain. *PLoS Comput. Biol.* **13**, e1005517 (2017).
86. San-Miguel, A. et al. Deep phenotyping unveils hidden traits and genetic relations in subtle mutants. *Nat. Commun.* **7**, 12990 (2016).
87. Peng, H., Ruan, Z., Atasoy, D. & Sternson, S. Automatic reconstruction of 3D neuron structures using a graph-augmented deformable model. *Bioinformatics* **26**, i38–46 (2010).
88. Moore, B. T., Jordan, J. M. & Baugh, L. R. WormSizer: high-throughput analysis of nematode size and shape. *PLoS One* **8**, e57142 (2013).
89. Wang, M. F. Z. & Fernandez-Gonzalez, R. (Machine-)learning to analyze in vivo microscopy: support vector machines. *Biochim. Biophys. Acta Proteins Proteom.* **1865**, 1719–1727 (2017).
90. White, A. G. et al. DevStaR: high-throughput quantification of *C. elegans* developmental stages. *IEEE Trans. Med. Imaging* **32**, 1791–1803 (2013).
91. Zhan, M. et al. Automated processing of imaging data through multi-tiered classification of biological structures illustrated using *Caenorhabditis elegans*. *PLoS Comput. Biol.* **11**, e1004194 (2015).
92. Entchev, E. V. et al. A gene-expression-based neural code for food abundance that modulates lifespan. *Elife* **4**, e06259 (2015).
93. Hakim, A. et al. WorMachine: machine learning-based phenotypic analysis tool for worms. *BMC Biol.* **16**, 8 (2018).
94. Zacharias, A. L. & Murray, J. I. Combinatorial decoding of the invariant *C. elegans* embryonic lineage in space and time. *Genesis* **54**, 182–197 (2016).
95. Fire, A. A four-dimensional digital image archiving system for cell lineage tracing and retrospective embryology. *Comput. Appl. Biosci.* **10**, 443–447 (1994).
96. Thomas, C., DeVries, P., Hardin, J. & White, J. Four-dimensional imaging: computer visualization of 3D movements in living specimens. *Science* **273**, 603–607 (1996).
97. Sonnichsen, B. et al. Full-genome RNAi profiling of early embryogenesis in *Caenorhabditis elegans*. *Nature* **434**, 462–469 (2005).
98. Gunsalus, K. C. et al. Predictive models of molecular machines involved in *Caenorhabditis elegans* early embryogenesis. *Nature* **436**, 861–865 (2005).
99. Bao, Z. et al. Automated cell lineage tracing in *Caenorhabditis elegans*. *Proc. Natl Acad. Sci. USA* **103**, 2707–2712 (2006).
100. Dzyubachyk, O., Jelier, R., Lehner, B., Niessen, W. & Meijering, E. Model-based approach for tracking embryogenesis in *Caenorhabditis elegans* fluorescence microscopy data. *Conf. Proc. IEEE Eng. Med. Biol. Soc.* **2009**, 5356–5359 (2009).
101. Giurumescu, C. A. et al. Quantitative semi-automated analysis of morphogenesis with single-cell resolution in complex embryos. *Development* **139**, 4271–4279 (2012).
102. Hunt-Newbury, R. et al. High-throughput in vivo analysis of gene expression in *Caenorhabditis elegans*. *PLoS Biol.* **5**, e237 (2007).
103. Murray, J. I. et al. Automated analysis of embryonic gene expression with cellular resolution in *C. elegans*. *Nat. Methods* **5**, 703–709 (2008).
104. Murray, J. I. et al. Multidimensional regulation of gene expression in the *C. elegans* embryo. *Genome Res.* **22**, 1282–1294 (2012).
105. Moore, J. L., Du, Z. & Bao, Z. Systematic quantification of developmental phenotypes at single-cell resolution during embryogenesis. *Development* **140**, 3266–3274 (2013).
106. Boeck, M. E. et al. Specific roles for the GATA transcription factors *end-1* and *end-3* during *C. elegans* E-lineage development. *Dev. Biol.* **358**, 345–355 (2011).
107. Du, Z. et al. The regulatory landscape of lineage differentiation in a metazoan embryo. *Dev. Cell.* **34**, 592–607 (2015).
108. Du, Z., Santella, A., He, F., Tiongson, M. & Bao, Z. De novo inference of systems-level mechanistic models of development from live-imaging-based phenotype analysis. *Cell* **156**, 359–372 (2014).
109. Ho, V. W. et al. Systems-level quantification of division timing reveals a common genetic architecture controlling asynchrony and fate asymmetry. *Mol. Syst. Biol.* **11**, 814 (2015).
110. Krüger, A. V. et al. Comprehensive single cell-resolution analysis of the role of chromatin regulators in early *C. elegans* embryogenesis. *Dev. Biol.* **398**, 153–162 (2015).
111. Keil, W., Kutscher, L. M., Shaham, S. & Siggia, E. D. Long-term high-resolution imaging of developing *C. elegans* larvae with microfluidics. *Dev. Cell.* **40**, 202–214 (2017).
112. Crane, M. M., Chung, K. & Lu, H. Computer-enhanced high-throughput genetic screens of *C. elegans* in a microfluidic system. *Lab. Chip* **9**, 38–40 (2009).
113. Uno, M. & Nishida, E. Lifespan-regulating genes in *C. elegans*. *NPJ. Aging Mech. Dis.* **2**, 16010 (2016).
114. Sutphin, G. L. & Kaeberlein, M. *Measuring Caenorhabditis elegans life span on solid media. J/of Vis Exp.* **12**, e1152 (2009).
115. Mathew, M. D., Mathew, N. D. & Ebert, P. R. WormScan: a technique for high-throughput phenotypic analysis of *Caenorhabditis elegans*. *PLoS One* **7**, e33483 (2012).
116. Stroustrup, N. et al. The *Caenorhabditis elegans* lifespan machine. *Nat. Methods* **10**, 665–670 (2013).
117. Stroustrup, N. et al. The temporal scaling of *Caenorhabditis elegans* ageing. *Nature* **530**, 103–107 (2016).
118. Rea, S. L., Wu, D., Cypser, J. R., Vaupel, J. W. & Johnson, T. E. A stress-sensitive reporter predicts longevity in isogenic populations of *Caenorhabditis elegans*. *Nat. Genet.* **37**, 894–898 (2005).
119. Zhang, W. B. et al. Extended twilight among isogenic *C. elegans* causes a disproportionate scaling between lifespan and health. *Cell Syst.* **3**, 333–345. e334 (2016).
120. Kapahi, P., Kaeberlein, M. & Hansen, M. Dietary restriction and lifespan: lessons from invertebrate models. *Ageing Res. Rev.* **39**, 3–14 (2017).
121. Lucanic, M. et al. Chemical activation of a food deprivation signal extends lifespan. *Aging Cell* **15**, 832–841 (2016).
122. Hullinger, R. & Puglielli, L. Molecular and cellular aspects of age-related cognitive decline and Alzheimer's disease. *Behav. Brain Res.* **322**, 191–205 (2017).

123. Arey, R. N. & Murphy, C. T. Conserved regulators of cognitive aging: from worms to humans. *Behav. Brain Res.* **322**, 299–310 (2017).
124. Bazopoulou, D., Chaudhury, A. R., Pantazis, A. & Chronis, N. An automated compound screening for anti-aging effects on the function of *C. elegans* sensory neurons. *Sci. Rep.* **7**, 9403 (2017).
125. Markaki, M. & Tavernarakis, N. Modeling human diseases in *Caenorhabditis elegans*. *Biotechnol. J.* **5**, 1261–1276 (2010).
126. Gosai, S. J. et al. Automated high-content live animal drug screening using *C. elegans* expressing the aggregation prone serpin α1-antitrypsin Z. *PLoS One* **5**, e15460 (2010).
127. O'Reilly, L. P. et al. A genome-wide RNAi screen identifies potential drug targets in a *C. elegans* model of α1-antitrypsin deficiency. *Hum. Mol. Genet.* **23**, 5123–5132 (2014).
128. Morley, J. F., Brignull, H. R., Weyers, J. J. & Morimoto, R. I. The threshold for polyglutamine-expansion protein aggregation and cellular toxicity is dynamic and influenced by aging in *Caenorhabditis elegans*. *Proc. Natl Acad. Sci. USA* **99**, 10417–10422 (2002).
129. Mondal, S. et al. Large-scale microfluidics providing high-resolution and high-throughput screening of *Caenorhabditis elegans* poly-glutamine aggregation model. *Nat. Commun.* **7**, 13023 (2016).
130. Samara, C. et al. Large-scale in vivo femtosecond laser neurosurgery screen reveals small-molecule enhancer of regeneration. *Proc. Natl Acad. Sci. U S A* **107**, 18342–18347 (2010).
131. Mathew, M. D. et al. Using *C. elegans* forward and reverse genetics to identify new compounds with anthelmintic activity. *PLoS Negl. Trop. Dis.* **10**, e0005058 (2016).
132. Partridge, F. A. et al. An automated high-throughput system for phenotypic screening of chemical libraries on *C. elegans* and parasitic nematodes. *Int. J. Parasitol. Drugs Drug. Resist.* **8**, 8–21 (2018).
133. Partridge, F. A. et al. Dihydrobenz[e][1,4]oxazepin-2(3H)-ones, a new anthelmintic chemotype immobilising whipworm and reducing infectivity. *in vivo. PLoS Negl. Trop. Dis.* **11**, e0005359 (2017).
134. Sykiotis, G. P. & Bohmann, D. Stress-activated cap'n'collar transcription factors in aging and human disease. *Sci. Signal.* **3**, re3 (2010).
135. Leung, C. K., Deonarine, A., Strange, K. & Choe, K. P. High-throughput screening and biosensing with fluorescent *C. elegans* strains. *J. Vis. Exp.* **51**, 2745 (2011).
136. Leung, C. K. et al. An ultra high-throughput, whole-animal screen for small molecule modulators of a specific genetic pathway in *Caenorhabditis elegans*. *PLoS One* **8**, e62166 (2013).
137. Abraham, M. C., Lu, Y. & Shaham, S. A morphologically conserved nonapoptotic program promotes linker cell death in *Caenorhabditis elegans*. *Dev. Cell* **12**, 73–86 (2007).
138. Schwendeman, A. R. & Shaham, S. A high-throughput small molecule screen for *C. elegans* .inker cell death inhibitors. *PLoS One* **11**, e0164595 (2016).
139. Pierce-Shimomura, J. T., Morse, T. M. & Lockery, S. R. The fundamental role of pirouettes in *Caenorhabditis elegans* chemotaxis. *J. Neurosci.* **19**, 9557–9569 (1999).
140. Cronin, C. J. et al. An automated system for measuring parameters of nematode sinusoidal movement. *BMC Genet.* **6**, 5 (2005).
141. Yemini, E., Jucikas, T., Grundy, L. J., Brown, A. E. & Schafer, W. R. A database of *Caenorhabditis elegans* behavioral phenotypes. *Nat. Methods* **10**, 877–879 (2013).
142. Chronis, N., Zimmer, M. & Bargmann, C. I. Microfluidics for in vivo imaging of neuronal and behavioral activity in *Caenorhabditis elegans*. *Nat. Methods* **4**, 727–731 (2007).
143. Feng, Z., Cronin, C. J., Wittig, J. H., Sternberg, P. W. & Schafer, W. R. An imaging system for standardized quantitative analysis of *C. elegans* behavior. *BMC Bioinformatics* **5**, 115 (2004).
144. Swierczek, N. A., Giles, A. C., Rankin, C. H. & Kerr, R. A. High-throughput behavioral analysis in *C. elegans*. *Nat. Methods* **8**, 592–598 (2011).
145. Itskovits, E., Levine, A., Cohen, E. & Zaslaver, A. A multi-animal tracker for studying complex behaviors. *BMC Biol.* **15**, 29 (2017).
146. Restif, C. et al. CeleST: computer vision software for quantitative analysis of *C. elegans* swim behavior reveals novel features of locomotion. *PLoS Comput. Biol.* **10**, e1003702 (2014).
147. Winter, P.B. et al. A network approach to discerning the identities of *C. elegans* in a free moving population. *Sci. Rep*. **6** (2016).
148. Perez-Escudero, A., Vicente-Page, J., Hinz, R. C., Arganda, S. & de Polavieja, G. G. idTracker: tracking individuals in a group by automatic identification of unmarked animals. *Nat. Methods* **11**, 743–748 (2014).
149. Perni, M. et al. Massively parallel *C. elegans* tracking provides multi-dimensional fingerprints for phenotypic discovery. *J. Neurosci. Methods* **306**, 57–67 (2018).
150. Yu, H. et al. Systematic profiling of *Caenorhabditis elegans* locomotive behaviors reveals additional components in G-protein Gαq signaling. *Proc. Natl Acad. Sci. USA* **110**, 11940–11945 (2013).
151. Ghosh, R., Mohammadi, A., Kruglyak, L. & Ryu, W. S. Multiparameter behavioral profiling reveals distinct thermal response regimes in *Caenorhabditis elegans*. *BMC Biol* **10**, 85 (2012).
152. McGrath, P. T. et al. Quantitative mapping of a digenic behavioral trait implicates globin variation in *C. elegans* sensory behaviors. *Neuron* **61**, 692–699 (2009).
153. Stephens, G. J., Johnson-Kerner, B., Bialek, W. & Ryu, W. S. Dimensionality and dynamics in the behavior of *C. elegans*. *PLoS Comput. Biol.* **4**, e1000028 (2008).
154. Brown, A. E., Yemini, E. I., Grundy, L. J., Jucikas, T. & Schafer, W. R. A dictionary of behavioral motifs reveals clusters of genes affecting *Caenorhabditis elegans* locomotion. *Proc. Natl Acad. Sci. USA* **110**, 791–796 (2013).
155. Sengupta, P. The belly rules the nose: feeding state-dependent modulation of peripheral chemosensory responses. *Curr. Opin. Neurobiol.* **23**, 68–75 (2013).
156. Calhoun, A. J. et al. Neural mechanisms for evaluating environmental variability in *Caenorhabditis elegans*. *Neuron* **86**, 428–441 (2015).
157. Calhoun, A. J., Chalasani, S. H. & Sharpee, T. O. Maximally informative foraging by *Caenorhabditis elegans*. *Elife* **3**, e04220 (2014).
158. Roberts, W. M. et al. A stochastic neuronal model predicts random search behaviors at multiple spatial scales in *C. elegans*. *Elife* **5**, e12572 (2016).
159. McCloskey, R. J., Fouad, A. D., Churgin, M. A. & Fang-Yen, C. Food responsiveness regulates episodic behavioral states in *Caenorhabditis elegans*. *J. Neurophysiol.* **117**, 1911–1934 (2017).
160. Churgin, M. A., McCloskey, R. J., Peters, E. & Fang-Yen, C. Antagonistic serotonergic and octopaminergic neural circuits mediate food-dependent locomotory behavior in *Caenorhabditis elegans*. *J. Neurosci.* **37**, 7811–7823 (2017).
161. Stern, S., Kirst, C. & Bargmann, C. I. Neuromodulatory control of long-term behavioral patterns and individuality across development. *Cell* **171**, 1649–1662.e10 (2017).
162. Bargmann, C. I. Genetic and cellular analysis of behavior in *C. elegans*. *Annu. Rev. Neurosci.* **16**, 47–71 (1993).
163. Gordus, A., Pokala, N., Levy, S., Flavell, S. W. & Bargmann, C. I. Feedback from network states generates variability in a probabilistic olfactory circuit. *Cell* **161**, 215–227 (2015).
164. Cho, Y., Zhao, C. L. & Lu, H. Trends in high-throughput and functional neuroimaging in *Caenorhabditis elegans*. *Wiley Interdiscip. Rev. Syst. Biol. Med.* **9**, e1376 (2017).
165. Kato, S. et al. Global brain dynamics embed the motor command sequence of *Caenorhabditis elegans*. *Cell* **163**, 656–669 (2015).
166. Venkatachalam, V. et al. Pan-neuronal imaging in roaming *Caenorhabditis elegans*. *Proc. Natl Acad. Sci. USA* **113**, E1082–1088 (2016).
167. Nguyen, J. P. et al. Whole-brain calcium imaging with cellular resolution in freely behaving *Caenorhabditis elegans*. *Proc Natl Acad. Sci. U S A* **113**, E1074–1081 (2016).
168. Nichols, A. L. A., Eichler, T., Latham, R. & Zimmer, M. A global brain state underlies *C. elegans* sleep behavior. *Science* **356**, eaam6851 (2017).
169. Eyer, K. et al. Single-cell deep phenotyping of IgG-secreting cells for high-resolution immune monitoring. *Nat. Biotechnol.* **35**, 977–982 (2017).
170. Crall, J. D. et al. Neonicotinoid exposure disrupts bumblebee nest behavior, social networks, and thermoregulation. *Science* **362**, 683–686 (2018).
171. Allalou, A., Wu, Y., Ghannad-Rezaie, M., Eimon, P. M. & Yanik, M. F. Automated deep-phenotyping of the vertebrate brain. *Elife* **6**, e23379 (2017).
172. Cheng, K. C., Xin, X., Clark, D. P. & La Riviere, P. Whole-animal imaging, gene function, and the Zebrafish phenome project. *Curr. Opin. Genet. Dev.* **21**, 620–629 (2011).
173. Hur, M. et al. MicroCT-based phenomics in the zebrafish skeleton r eveals virtues of deep phenotyping in a distributed organ system. *Elife* **6**, e26014 (2017).

Acknowledgements

We thank K.E. Bates, D.A. Porto and T. Rouse for their suggestions on relevant literature, and the US National Institutes of Health (grants AG056436, DC015652, NS096581, GM088333, EB021676, EB020424 and GM10896) and National Science Foundation (grants 1707401 and 1764406) for funding support.

Competing interests

The authors declare no competing interests.

Additional information

Reprints and permissions information is available at www.nature.com/reprints.

Correspondence should be addressed to H.L.

Publisher's note: Springer Nature remains neutral with regard to jurisdictional claims in published maps and institutional affiliations.